Study of off-diagonal disorder using the typical medium dynamical cluster approximation

H. Terletska,[1,2,*] C. E. Ekuma,[1,2] C. Moore,[1,2] K.-M. Tam,[1,2] J. Moreno,[1,2] and M. Jarrell[1,2,†]
[1]*Department of Physics & Astronomy, Louisiana State University, Baton Rouge, Louisiana 70803, USA*
[2]*Center for Computation & Technology, Louisiana State University, Baton Rouge, Louisiana 70803, USA*
(Received 3 June 2014; published 26 September 2014)

We generalize the typical medium dynamical cluster approximation and the local Blackman, Esterling, and Berk method for systems with off-diagonal disorder. Using our extended formalism we perform a systematic study of the effects of nonlocal disorder-induced correlations and off-diagonal disorder on the density of states and the mobility edge of the Anderson localized states. We apply our method to the three-dimensional Anderson model with configuration-dependent hopping and find fast convergence with modest cluster sizes. Our results are in good agreement with the data obtained using exact diagonalization and the transfer-matrix and kernel polynomial methods.

DOI: 10.1103/PhysRevB.90.094208 PACS number(s): 71.27.+a, 02.70.−c, 71.10.Fd, 71.23.An

I. INTRODUCTION

Disorder, which is inevitably present in most materials, can dramatically affect their properties [1,2]. It can lead to changes in their electronic structure and transport. One of the most interesting effects of disorder is the spatial confinement of charge carriers due to coherent backscattering off random impurities, which is known as Anderson localization [3,4]. Despite progress over the past decades, the subject of Anderson localization remains an active area of research. The lack of quantitative analytical results has meant that numerical investigations [5–11] have provided a significant role in understanding the Anderson transition [12–14].

The simplest model used to study the effects of disorder in materials is a single-band tight-binding model with a random on-site disorder potential [15]. Such a model is justified when the disorder is introduced by substitutional impurities as in a binary alloy. The substitution of host atoms by impurities only leads to changes in the local potential on the substitutional site and, on average, does not affect the neighbors [15,16]. In this situation, the disorder appears only in the diagonal terms of the Hamiltonian and hence is referred to as diagonal disorder. However, when the bandwidth of the dopant is very different from the one of the pure host, such substitution results not only in the change in the local potential, but also in affecting the neighboring sites [15]. Consequently, a simple model to capture such effects should include both random local potentials and random hopping amplitudes which depend on the occupancy of the sites. The dependence of the hopping amplitude on the disorder configuration is usually referred to as off-diagonal disorder. It is apparent that a proper theoretical description of realistic disordered materials [15,17–20] (for, e.g., many substitutionally disordered alloys and disordered ferromagnets) requires the inclusion of both diagonal and off-diagonal randomnesses. Although the role of the diagonal disorder has been extensively studied over the past several decades [21], the effect of off-diagonal disorder is not well studied, although the effect is expected to be different. It has been shown [18,22] that off-diagonal randomness can lead to the delocalization of the states near the band center. Also recently, there has been a growing interest in the effect of the off-diagonal randomness in graphene systems where studies show that different types of disorder can induce different localization behaviors [23–25].

The coherent-potential approximation (CPA) is a widely used single-site mean-field theory for systems with strictly diagonal disorder [16]. Blackman, Esterling, and Berk (BEB) [26] have extended the CPA to systems with off-diagonal disorder. However, being single-site approximations, the CPA and the BEB theories neglect all disorder-induced nonlocal correlations.

There have been a number of attempts to develop systematic nonlocal extensions to the CPA. These include cluster extensions, such as the molecular coherent-potential approximation (MCPA) [27,28], the dynamical cluster approximation (DCA) [29–31], etc. Self-consistent mean-field studies of off-diagonal disorder have been conducted by a number of authors [28,32–34]. However, all these studies have been performed at the local single-site BEB level. To include the effects of off-diagonal disorder, Gonis and Garland [27] extended the molecular CPA, which uses a self-consistently embedded finite-size cluster to capture nonlocal corrections to the CPA. However, they criticized the MCPA for violating translational invariance and other critical properties of a valid quantum cluster theory [15,35]. In order to take into account such nonlocal effects on off-diagonal-disorder models while maintaining translational invariance, we extend the BEB formalism using the DCA scheme [29–31].

Although the CPA, DCA, and BEB have shown to be successful self-consistent mean-field theories for the quantitative description of the density of states (DOS) and electronic structure of disordered systems, they cannot properly address the physics of Anderson localization. These mean-field approaches describe the effective medium using the average density of states, which is not critical at the transition [12,35–37]. Thus, theories which rely on such averaged quantities will fail to properly characterize Anderson localization. As noted by Anderson, the probability distribution of the local density of states must be considered, focusing on the most probable or the *typical* value [3,38]. Close to the Anderson transition, the distribution is found to have very long tails

*terletska.hannas@gmail.com
†jarrellphysics@gmail.com

characteristic of a log-normal distribution [10,39,40]. In fact, the distribution is log-normal up to ten orders of magnitude [41], and so the typical value [40,42–44] is the geometrical mean. Based on this idea, Dobrosavljević *et al.* [45] formulated a single-site typical medium theory (TMT) for the Anderson localization. This approximation gives a qualitative description of the Anderson localization in three dimensions. However, it fails to properly describe the trajectory of the mobility edge (which separates the extended and localized states) as it neglects nonlocal corrections and so does not include the effects of coherent backscattering [46]. It also underestimates considerably the critical strength of the disorder at which the localization happens. In addition, TMT is only formulated for diagonal disorder.

Recently, by employing the DCA within the typical medium analysis, we developed a systematic typical medium dynamical cluster approximation (TMDCA) formalism [35]. The TMDCA provides an accurate description of the Anderson localization transition for modest cluster sizes in three-dimensional models with diagonal disorder while recovering the TMT for a one-site cluster. In this paper, we generalize our recently proposed TMDCA scheme to address the question of electron localization in systems with both diagonal and off-diagonal disorders.

In this paper, to go beyond the local single-site CPA-like level of the BEB formalism, we employ the DCA [29–31] scheme which systematically incorporates nonlocal spatial correlation effects. We first present an extension of the DCA for systems with both diagonal and off-diagonal disorders. Comparing our single-site and finite cluster results, we demonstrate the effect of nonlocal correlations on the density of states and the self-energy.

Here we develop a typical medium formalism for systems with off-diagonal disorder. So far, the typical medium analysis has been applied to systems with only diagonal disorder [35,45]. In this paper, we develop a typical medium dynamical cluster approximation formalism capable of characterizing the localization transition in systems with both diagonal and off-diagonal disorders. We perform a systematic study of the effects of nonlocal correlations and off-diagonal randomness on the density of states and electron localization. By comparing single-site and finite cluster results for the typical density of states and the extracted mobility edges, we demonstrate the necessity of including the nonlocal multisite effects for proper and quantitative characterization of the localization transition. The results of our calculations are compared with the ones obtained with other numerical methods for finite-size lattices, including exact diagonalization, kernel polynomial, and transfer-matrix methods.

The paper is organized as follows: Following the Introduction in Sec. I we present the model and describe the details of the formalism we used in Sec. II. In Sec. III A we present our results of the average density of states for both diagonal and off-diagonal-disorder cases. In Sec. III B we consider the effects of diagonal and off-diagonal disorders on the typical density of states, from which we extract the mobility edges and construct a complete phase diagram in the disorder-energy parameter space. We summarize and discuss future directions in Sec. IV.

II. FORMALISM

A. Dynamical cluster approximation for off-diagonal disorder

The simplest model widely used to study disordered systems is the single-band tight-binding Hamiltonian,

$$H = -\sum_{\langle i,j\rangle} t_{ij}(c_i^\dagger c_j + \text{H.c.}) + \sum_i v_i n_i, \tag{1}$$

where disorder is modeled by a local potential v_i which is a random variable with probability distribution function $P(v_i)$. We will focus on the binary disorder case where some host A atoms are substituted with B impurities with a probability distribution function of the form

$$P(v_i) = c_A\delta(v_i - V_A) + c_B\delta(v_i - V_B), \tag{2}$$

where $c_B = 1 - c_A$. For the diagonal-disorder case when the bandwidth of the pure host A is about the same as the bandwidth of the B system, such substitution results only in a change in the local potential v_i at the replaced site i. This corresponds to changes in the diagonal elements of the Hamiltonian. In this case it is assumed that substitution of impurity atoms on average has no effect on hopping amplitudes to the neighboring atoms.

For systems with off-diagonal disorder, the randomness is introduced not only locally in the random diagonal potential v_i, but also through the hopping amplitudes. To model this, BEB [26] introduced the disorder-configuration-dependent hopping amplitude of electrons t_{ij} as

$$\begin{aligned} t_{ij} &= t_{ij}^{AA}, \quad \text{if} \quad i \in A,\ j \in A,\\ t_{ij} &= t_{ij}^{BB}, \quad \text{if} \quad i \in B,\ j \in B,\\ t_{ij} &= t_{ij}^{AB}, \quad \text{if} \quad i \in A,\ j \in B,\\ t_{ij} &= t_{ij}^{BA}, \quad \text{if} \quad i \in B,\ j \in A, \end{aligned} \tag{3}$$

where t_{ij} depends on the type of ion occupying sites i and j. For off-diagonal-disorder BEB [26] showed the scalar CPA equation becomes a 2×2 matrix equation with corresponding AA, AB, BA, and BB matrix elements. In momentum space, if there is only near-neighbor hopping between all ions, the bare dispersion can be written as (the underbar denotes matrices)

$$\underline{\varepsilon_k} = \begin{pmatrix} t^{AA} & t^{AB} \\ t^{BA} & t^{BB} \end{pmatrix}\varepsilon_k, \tag{4}$$

where in three dimensions $\varepsilon_k = -2t[\cos(k_x) + \cos(k_y) + \cos(k_z)]$ with $4t = 1$ which sets our unit of energy and t^{AA}, t^{BB}, t^{AB}, and t^{BA} are unitless prefactors.

The BEB approach is local by construction, hence all nonlocal disorder-induced correlations are neglected [26]. In order to take into account nonlocal physics, we extend the BEB formalism to a finite cluster using the DCA scheme. Here in the following, we present the algorithm and details of our nonlocal DCA extension of the BEB formalism for off-diagonal disorder. Just as in the DCA scheme [31], the first Brillouin zone is divided into $N_c = L^D$ (D is the dimension, and L is the linear cluster size) coarse-grained cells with centers K surrounded by points $\tilde{k}$ within the cell so that an arbitrary $k = K + \tilde{k}$.

For a given DCA K-dependent effective medium hybridization $\underline{\Delta(K,\omega)}$ matrix we use an underline to denote a 2×2 matrix in momentum space),

$$\underline{\Delta(K,\omega)} = \begin{pmatrix} \Delta^{AA}(K,\omega) & \Delta^{AB}(K,\omega) \\ \Delta^{BA}(K,\omega) & \Delta^{BB}(K,\omega) \end{pmatrix}, \tag{5}$$

and we solve the cluster problem, usually in real space. For this we stochastically sample random configurations of the disorder potential V and calculate the corresponding cluster Green's function by inverting the $N_c \times N_c$ matrix, i.e.,

$$G_{ij} = (\omega\mathbb{I} - \overline{t}' - \Delta' - V)^{-1}_{ij}, \tag{6}$$

where V is a diagonal matrix for the disorder site potential. The primes stand for the configuration-dependent Fourier-transform (FT) components of the hybridization and hopping, respectively. I.e.,

$$\Delta'_{ij} = \begin{cases} \mathrm{FT}[\Delta^{AA}(K,\omega)], & \text{if} \quad i\in A,\ j\in A, \\ \mathrm{FT}[\Delta^{BB}(K,\omega)], & \text{if} \quad i\in B,\ j\in B, \\ \mathrm{FT}[\Delta^{AB}(K,\omega)], & \text{if} \quad i\in A,\ j\in B, \\ \mathrm{FT}[\Delta^{BA}(K,\omega)], & \text{if} \quad i\in B,\ j\in A, \end{cases} \tag{7a}$$

and

$$\overline{t}'_{ij} = \begin{cases} \mathrm{FT}[\overline{\epsilon}^{AA}(K)], & \text{if} \quad i\in A,\ j\in A, \\ \mathrm{FT}[\overline{\epsilon}^{BB}(K)], & \text{if} \quad i\in B,\ j\in B, \\ \mathrm{FT}[\overline{\epsilon}^{AB}(K)], & \text{if} \quad i\in A,\ j\in B, \\ \mathrm{FT}[\overline{\epsilon}^{BA}(K)], & \text{if} \quad i\in B,\ j\in A, \end{cases} \tag{7b}$$

with

$$\underline{\overline{\epsilon}(K)} = \begin{pmatrix} t^{AA} & t^{AB} \\ t^{BA} & t^{BB} \end{pmatrix} \frac{N_c}{N} \sum_{\tilde{k}} \varepsilon_k, \tag{7c}$$

where Δ'_{ij} and $\overline{t}'_{ij}$ are $N_c \times N_c$ real-space matrices (where N_c is the cluster size), and, e.g., $\mathrm{FT}[\Delta^{AA}(K,\omega)] = \sum_K \Delta^{AA}(K,\omega)e^{iK(r_i-r_j)}$. The hopping can be long ranged, but since they are coarse-grained quantities, they are effectively limited to the cluster. Physically, Δ'_{ij} represents the hybridization between sites i and j, which is configuration dependent. For example, the AA component of the hybridization corresponds to both A species occupying sites i and j, whereas the AB component means that site i is occupied by an A atom and site j by a B atom. The interpretation of the hopping matrix is the same as for the hybridization function.

In the next step, we perform averaging over the disorder $\langle(\cdots)\rangle$, and in doing so we reexpand the Green's function [Eq. (6)] into a $2N_c \times 2N_c$ matrix,

$$G_c(\omega)_{ij} = \begin{pmatrix} \langle G_c^{AA}(\omega)\rangle_{ij} & \langle G_c^{AB}(\omega)\rangle_{ij} \\ \langle G_c^{BA}(\omega)\rangle_{ij} & \langle G_c^{BB}(\omega)\rangle_{ij} \end{pmatrix}. \tag{8}$$

This may be performed by assigning the components according to the occupancy of sites i and j,

$$\begin{aligned} \left(G_c^{AA}\right)_{ij} &= (G_c)_{ij}, \quad \text{if} \quad i\in A,\ j\in A, \\ \left(G_c^{BB}\right)_{ij} &= (G_c)_{ij}, \quad \text{if} \quad i\in B,\ j\in B, \\ \left(G_c^{AB}\right)_{ij} &= (G_c)_{ij}, \quad \text{if} \quad i\in A,\ j\in B, \\ \left(G_c^{BA}\right)_{ij} &= (G_c)_{ij}, \quad \text{if} \quad i\in B,\ j\in A, \end{aligned} \tag{9}$$

with the other components being zero. Because only one of the four matrix elements is finite for each disorder configuration (each site can be occupied by either an A or a B atom), only the sum of the elements in Eq. (8) is normalized as a conventional Green's function.

Having formed the disorder-averaged cluster Green's function matrix, we then Fourier transform each component to K space (which also imposes translational symmetry) and construct the K-dependent disorder-averaged cluster Green's function matrix in momentum space,

$$\underline{G_c(K,\omega)} = \begin{pmatrix} G_c^{AA}(K,\omega) & G_c^{AB}(K,\omega) \\ G_c^{BA}(K,\omega) & G_c^{BB}(K,\omega) \end{pmatrix}. \tag{10}$$

Once the cluster problem is solved, we calculate the coarse-grained lattice Green's function matrix as

$$\begin{aligned} \underline{\overline{G}(K,\omega)} &= \begin{pmatrix} \overline{G}^{AA}(K,\omega) & \overline{G}^{AB}(K,\omega) \\ \overline{G}^{BA}(K,\omega) & \overline{G}^{BB}(K,\omega) \end{pmatrix} \\ &= \frac{N_c}{N} \sum_{\tilde{k}} [\underline{G_c(K,\omega)}^{-1} + \underline{\Delta(K,\omega)} - \underline{\varepsilon_k} + \underline{\overline{\epsilon}(K)}]^{-1}, \end{aligned} \tag{11}$$

here we use an overbar to denote the cluster coarse-grained quantities. It is important to note that each component of the Green's function matrix above does not have the normalization of a conventional, i.e., scalar, Green's function. Only the sum of the matrix components has the conventional normalization so that $\overline{G}(K,\omega) \sim 1/\omega$ with the total coarse-grained lattice Green's function being obtained as

$$\begin{aligned} \overline{G}(K,\omega) = \overline{G}^{AA}(K,\omega) + \overline{G}^{BB}(K,\omega) + \overline{G}^{AB}(K,\omega) \\ + \overline{G}^{BA}(K,\omega). \end{aligned} \tag{12}$$

Next, to construct the new DCA effective medium $\underline{\Delta(K,\omega)}$, we impose the BEB DCA (2×2) matrix self-consistency condition, requiring the disorder-averaged cluster and the coarse-grained lattice Green's functions to be equal

$$\underline{G_c(K,\omega)} = \underline{\overline{G}(K,\omega)}. \tag{13}$$

This is equivalent to a system of three coupled scalar equations,

$$\overline{G}^{AA}(K,\omega) = G_c^{AA}(K,\omega), \tag{14a}$$

$$\overline{G}^{BB}(K,\omega) = G_c^{BB}(K,\omega), \tag{14b}$$

and

$$\overline{G}^{AB}(K,\omega) = G_c^{AB}(K,\omega). \tag{14c}$$

Note $\overline{G}^{BA}(K,\omega) = \overline{G}^{AB}(K,\omega)$ automatically if $t^{AB} = t^{BA}$.

We then close our self-consistency loop by updating the corresponding hybridization functions for each component as

$$\begin{aligned} \Delta_n^{AA}(K,\omega) &= \Delta_o^{AA}(K,\omega) + \xi\left[G_c^{-1}(K,\omega)^{AA} - \overline{G}^{-1}(K,\omega)^{AA}\right] \\ \Delta_n^{BB}(K,\omega) &= \Delta_o^{BB}(K,\omega) + \xi\left[G_c^{-1}(K,\omega)^{BB} - \overline{G}^{-1}(K,\omega)^{BB}\right] \\ \Delta_n^{AB}(K,\omega) &= \Delta_o^{AB}(K,\omega) + \xi\left[G_c^{-1}(K,\omega)^{AB} - \overline{G}^{-1}(K,\omega)^{AB}\right] \\ \Delta_n^{BA}(K,\omega) &= \Delta_n^{AB}(K,\omega), \end{aligned} \tag{15}$$

where "o" and "n" denote old and new, respectively, and ξ is a linear mixing parameter $0 < \xi < 1$. We then iterate the above steps until convergence is reached.

There are two limiting cases of the above formalism which we carefully checked numerically. In the limit of $N_c = 1$, we should recover the original BEB result. Here the cluster Green's function loses its K dependence so that

$$\begin{pmatrix} G_c^{AA}(\omega) & 0 \\ 0 & G_c^{BB}(\omega) \end{pmatrix} = \frac{1}{N}\sum_k [\underline{G_c(\omega)}^{-1} + \underline{\Delta(\omega)} - \underline{\varepsilon(k)}]^{-1}, \tag{16}$$

which is the BEB self-consistency condition. Here we used that $\overline{\epsilon}(K) = 0$ for $N_c = 1$. The second limiting case is when there is only diagonal disorder so that $t^{AA} = t^{BB} = t^{AB} = 1$. In this case the above formalism reduces to the original DCA scheme. We have verified numerically both limits.

B. Typical medium theory with off-diagonal disorder

To address the issue of electron localization, we recently developed the TMDCA and applied it to the three-dimensional Anderson model [35]. In Ref. [35] we confirmed that the typical density of states vanishes for states which are localized and it is finite for extended states. In the following we generalize our TMDCA analysis to systems with off-diagonal disorder to address the question of localization and the mobility edge in such models.

First, we would like to emphasize that the crucial difference between the TMDCA [35] and the standard DCA [31] procedure is the way the disorder-averaged cluster Green's function is calculated. In the TMDCA analysis instead of using the algebraically averaged cluster Green's function in the self-consistency loop, we calculate the typical (geometrically) averaged cluster density of states,

$$\rho^c_{\rm typ}(K,\omega) = e^{(1/N_c)\sum_i \langle \ln\, \rho_{ii}(\omega)\rangle} \left\langle \frac{-\frac{1}{\pi}{\rm Im}\, G_c(K,\omega)}{\frac{1}{N_c}\sum_i \left[-\frac{1}{\pi}{\rm Im}\, G_{ii}(\omega)\right]} \right\rangle, \tag{17}$$

with the geometric averaging being performed over the local density of states $\rho_{ii}(\omega) = -\frac{1}{\pi}{\rm Im}\, G_{ii}(w)$ only. Using this $\rho^c_{\rm typ}(K,\omega)$ the cluster-averaged typical Green's function is constructed via a Hilbert transform,

$$G_c(K,\omega) = \int d\omega' \frac{\rho^c_{\rm typ}(K,\omega')}{\omega - \omega'}. \tag{18}$$

In the presence of off-diagonal disorder, following BEB, the typical density of states becomes a 2×2 matrix, which we define as

$$\underline{\rho^c_{\rm typ}(K,\omega)} = \exp\left(\frac{1}{N_c}\sum_{i=1}^{N_c}\langle \ln\, \rho_{ii}(\omega)\rangle\right) \begin{pmatrix} \left\langle \frac{-\frac{1}{\pi}{\rm Im}\, G_c^{AA}(K,\omega)}{\frac{1}{N_c}\sum_{i=1}^{N_c}\left(-\frac{1}{\pi}{\rm Im}\, G_{ii}(\omega)\right)} \right\rangle & \left\langle \frac{-\frac{1}{\pi}{\rm Im}\, G_c^{AB}(K,\omega)}{\frac{1}{N_c}\sum_{i=1}^{N_c}\left(-\frac{1}{\pi}{\rm Im}\, G_{ii}(\omega)\right)} \right\rangle \\ \left\langle \frac{-\frac{1}{\pi}{\rm Im}\, G_c^{BA}(K,w)}{\frac{1}{N_c}\sum_{i=1}^{N_c}\left(-\frac{1}{\pi}{\rm Im}\, G_{ii}(\omega)\right)} \right\rangle & \left\langle \frac{-\frac{1}{\pi}{\rm Im}\, G_c^{BB}(K,\omega)}{\frac{1}{N_c}\sum_{i=1}^{N_c}\left(-\frac{1}{\pi}{\rm Im}\, G_{ii}(\omega)\right)} \right\rangle \end{pmatrix}. \tag{19}$$

Here the scalar prefactor depicts the local typical (geometrically averaged) density of states (TDOS), whereas the matrix elements are linearly averaged over the disorder. Also notice that the cluster Green's function $(\underline{G_c})_{ij}$ and its components G_c^{AA}, G_c^{BB}, and G_c^{AB} are defined in the same way as in Eqs. (6)–(10).

In the next step, we construct the cluster average Green's function $G_c(K,\omega)$ by performing a Hilbert transform for each component,

$$\underline{G_c(K,\omega)} = \begin{pmatrix} \int d\omega' \frac{\rho^{AA}_{\rm typ}(K,\omega')}{\omega-\omega'} & \int d\omega' \frac{\rho^{AB}_{\rm typ}(K,\omega')}{\omega-\omega'} \\ \int d\omega' \frac{\rho^{BA}_{\rm typ}(K,\omega')}{\omega-\omega'} & \int d\omega' \frac{\rho^{BB}_{\rm typ}(K,\omega')}{\omega-\omega'} \end{pmatrix}. \tag{20}$$

Once the disorder-averaged cluster Green's function $G_c(K,\omega)$ is obtained from Eq. (20), the self-consistency steps are the same as in the procedure for the off-diagonal-disorder DCA described in the previous section: We calculate the coarse-grained lattice Green's function using Eq. (11), which is then used to update the hybridization function with the effective medium via Eq. (15).

The above set of equations provides us with the generalization of the TMDCA scheme for both diagonal and off-diagonal disorders, which we test numerically in the following sections. Also notice that for $N_c = 1$ with only diagonal disorder ($t^{AA} = t^{BB} = t^{AB} = t^{BA}$) the above procedure reduces to the local TMT scheme. In this case, the diagonal elements of the matrix in Eq. (19) will contribute c_A and c_B, respectively, with the off-diagonal elements being zero (for $N_c = 1$ the off-diagonal terms vanish because a given site can only be either A or B). Hence, the typical density reduces to the local scalar prefactor only, which has exactly the same form as in the local TMT scheme.

Another limit of the proposed ansatz for the typical density of states of Eq. (19) is obtained at small disorder. In this case, the TMDCA reduces to the DCA for off-diagonal disorder as the geometrically averaged local prefactor term numerically cancels with the contribution from the linearly averaged local term in the denominator of Eq. (19).

Finally, we also want to mention that the developed cluster TMDCA fulfills all the essential requirements expected of a successful cluster theory [15] including causality and translational invariance.

We note that in our formalism, instead of performing the very expensive enumeration of the disorder configurations which scales as 2^{Nc}, we instead perform a stochastic sampling of the disorder configurations which greatly reduces the computational cost enabling us to study larger systems. Larger system sizes need fewer realizations. Since the convergence criterion is achieved when the TDOS ($\omega = 0$) does not fluctuate anymore with iteration number, within the error bars, our computational cost does not even scale as N_c. For a typical $N_c = 64$ size cluster, about 500 disorder realizations are needed to get reliable data, and this number decreases with increasing cluster size.

III. RESULTS AND DISCUSSION

To illustrate the generalized DCA and TMDCA algorithms described above, we present our results for the effects of diagonal and off-diagonal disorders in a generalized Anderson Hamiltonian [Eq. (1)] for a three-dimensional system with binary disorder distribution ($V_A = -V_B$) and random hopping ($t^{AA} \neq t^{BB}$, $t^{AB} = t^{BA}$) with other parameters as specified. The results are presented and are discussed in Secs. III A and III B.

A. DCA results for diagonal and off-diagonal disorders

The effect of off-diagonal disorder on the average DOS calculated within the DCA for a cubic cluster ($N_c = 4^3$) is presented in Fig. 1. The DOS we present in our results is a local density of states calculated as

$$\mathrm{DOS}(\omega) = -\frac{1}{\pi N_c}\sum_{K=1}^{N_c}[\mathrm{Im}\,\overline{G}^{AA}(K,\omega) + \mathrm{Im}\,\overline{G}^{AB}(K,\omega) + \mathrm{Im}\,\overline{G}^{BA}(K,\omega) + \mathrm{Im}\,\overline{G}^{BB}(K,\omega)]. \quad (21)$$

Notice that our DCA procedure for $N_c = 1$ reduces to the original CPA-like BEB. For a fixed concentration $c_A = 0.5$, we examine the effects of off-diagonal disorder at two fixed values of the diagonal-disorder potential $V_A = 0.4$ (below the split-band limit) and $V_A = 0.9$ (above the split-band limit). The off-diagonal randomness is modeled by changes in the hopping amplitudes t^{AA},t^{BB} with $t^{AB} = 0.5(t^{AA} + t^{BB})$. For a diagonal-disorder case (top panel of Fig. 1) with $t^{AA} = t^{BB} = t^{AB} = t^{BA}$ we have two sub-bands contributing equally to the total DOS; whereas as shown in the middle and bottom panels, the change in the strength of the off-diagonal disorder leads to dramatic changes in the DOS. An increase in the AA hopping results in the broadening of the AA sub-band with the development of a resonance peak at the BB sub-band. For this parameter range both the DCA ($N_c = 64$) and the CPA ($N_c = 1$) provide about the same results indicating that disorder-induced nonlocal correlations are negligible.

In Fig. 2 we show the average density of states calculated for fixed off-diagonal-disorder parameters and different diagonal-disorder potentials V_A. We again compare the local CPA ($N_c = 1$) and the DCA ($N_c = 4^3$) results. To benchmark our off-diagonal extension of the DCA, we also compare our results with those obtained from exact diagonalization. For small V_A, there is no difference between the CPA ($N_c = 1$) and the DCA ($N_c = 4^3$) results. As local potential V_A is increased, noticeable differences start to develop. We can see that for larger V_A a gap starts to open and is more dramatic in the CPA scheme; whereas in the DCA ($N_c = 4^3$) this gap is partially filled due to the incorporation of nonlocal intersite correlations which are missing in the CPA. Furthermore, the DOS obtained from the DCA procedure provides finer structures which are in basic agreement with

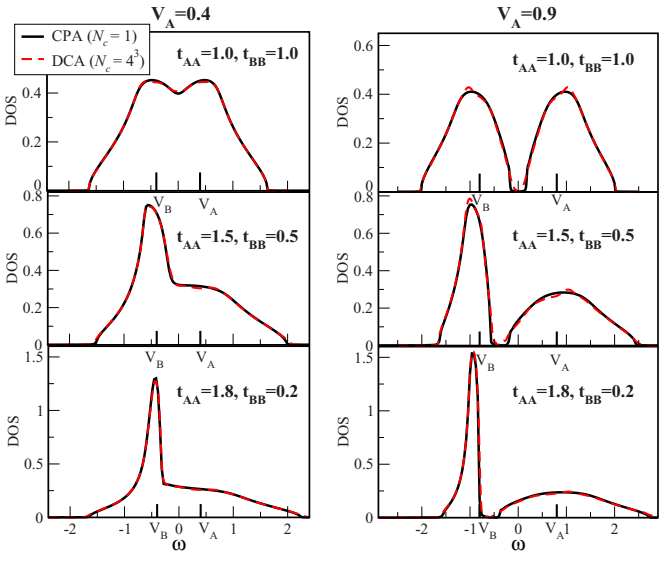

FIG. 1. (Color online) The effect of off-diagonal disorder on the average density of states calculated in the DCA scheme with $N_c = 4^3$. Our DCA results for $N_c = 1$ corresponds to a single-site CPA BEB scheme. We consider two values of local disorder potential below ($V_A = 0.4$) and above ($V_A = 0.9$) the band-split limit and examine the effect of changing the off-diagonal hopping strength (which amounts to a change in the nonlocal potential). We start with the diagonal-disorder case $t^{AA} = t^{BB} = t^{AB} = 1.0$ and then consider two off-diagonal-disorder cases: $t^{AA} = 1.5$, $t^{BB} = 0.5$ and $t^{AA} = 1.8$, $t^{BB} = 0.2$, respectively. We fix $t^{AB} = t^{BA} = 0.5(t^{AA} + t^{BB})$ and $c_A = 0.5$. For this parameter range of off-diagonal disorder, we do not observe a significant difference between the CPA ($N_c = 1$) and the DCA ($N_c = 4^3$) results indicating that nonlocal intersite correlations are weak.

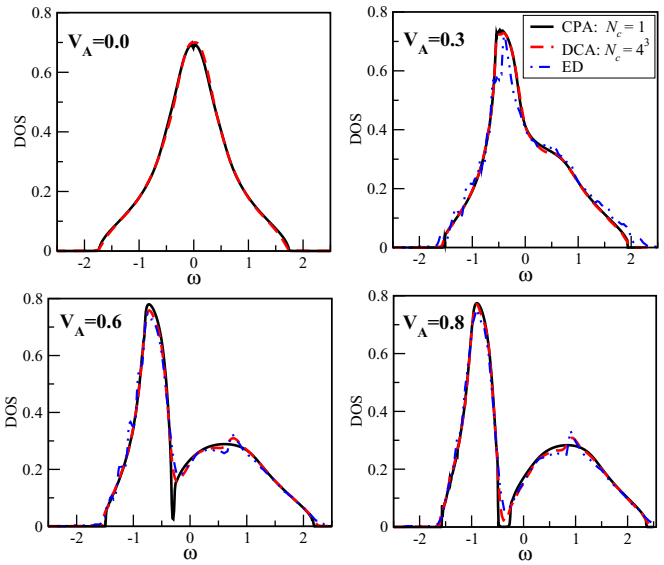

FIG. 2. (Color online) The effect on the average density of states of an increasing diagonal-disorder potential V_A for a fixed off-diagonal disorder calculated with our modified DCA scheme with $t^{AA} = 1.5$, $t^{BB} = 0.5$, $t^{AB} = 0.5(t^{AA} + t^{BB})$, and $c_A = 0.5$. Results are obtained for $N_c = 1$ (corresponding to the CPA) and $N_c = 4^3$ cluster sizes. We also compare our DCA average DOS with the DOS obtained using exact diagonalization (ED) for a 12^3 cubic lattice cluster with 48 disorder realizations. For ED results, we used a $\eta = 0.01$ broadening in frequency.

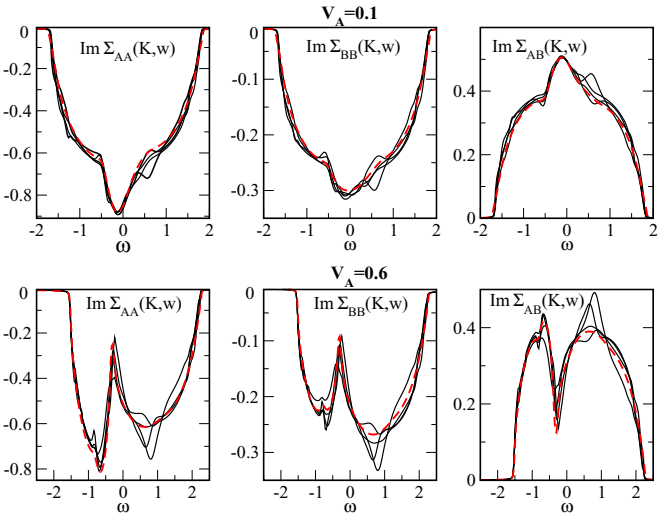

FIG. 3. (Color online) The imaginary part of the self-energy vs frequency ω for $N_c = 1$ (red dashed line) and $N_c = 4^3$ (solid lines) at various K momenta points: (0,0,0), (π,0,0), (π,π,0), and ($\pi/2$,$\pi/2$,$\pi/2$) for $V_A = 0.1$ (top) and $V_A = 0.6$ (bottom) diagonal-disorder potential with $t^{AA} = 1.5$, $t^{BB} = 0.5$, $t^{AB} = 0.5(t^{AA} + t^{BB})$, and $c_A = 0.5$. For small disorder $V_A = 0.1$, the self-energy for $N_c = 1$ is essentially the same as that of the various K points of the $N_c = 4^3$ cluster, indicating that nonlocal effects are negligible for such small disorder. For a larger value of the disorder $V_A = 0.6$, the single-site and the finite cluster data differ significantly, which illustrates that at larger disorder, the momentum dependence of the self-energy increases and becomes important.

the DOS calculated with exact diagonalization for a cluster of size $12 \times 12 \times 12$. The agreement we get with ED results is a good indication of the the accuracy of our extension of the DCA to off-diagonal disorder. The additional structures observed in the DOS for $N_c > 1$, which are absent in the CPA, are believed to be related to the local order in the environment of each site [15,31]. Notice that, although the DCA accounts for nonlocal backscattering effects which lead to the Anderson localization, the average local DOS does not capture the transition as it is not an order parameter for the Anderson localization.

To further illustrate the important effect of the nonlocal contributions from the cluster, we also show in Fig. 3 the imaginary part of the self-energy $\mathrm{Im}\,\Sigma(K,w)$ for $N_c = 1$ (dashed line) and for ($N_c = 4^3$) (solid lines) at different values of cluster momenta $K = (0,0,0)$, $(\pi,0,0)$, $(\pi,\pi,0)$, and $(\pi/2,\pi/2,\pi/2)$ for small $V_A = 0.1$ (top) and larger $V_A = 0.6$ (bottom) disorder potentials. At small disorder $V_A = 0.1$, there is a little momentum dependence for the $N_c = 4^3$ self-energy, and different K momenta curves practically fall on top of each other. The results for $N_c = 1$ and $N_c = 4^3$ are essentially the same, which indicates that for small disorder the CPA still presents a good approximation for the self-energy. On the other hand, for larger disorder $V_A = 0.6$ the $N_c = 1$ and $N_c = 4^3$ results differ significantly with the $N_c = 4^3$ self-energy having a noticeable momentum dependence, indicating that nonlocal correlations become more pronounced for larger disorder values.

B. Typical medium finite cluster analysis of diagonal and off-diagonal disorders Typical medium analysis of diagonal disorder

To characterize the Anderson localization transition, we now explore the TDOS calculated within our extension of the TMDCA presented in Sec. II B. In the typical medium analysis, the TDOS serves as the order parameter for the Anderson localization transition. In particular, the TDOS is finite for extended states and zero for states which are localized.

First we consider the behavior of the TDOS and compare it with the average DOS for diagonal disorder. In Fig. 4 we show

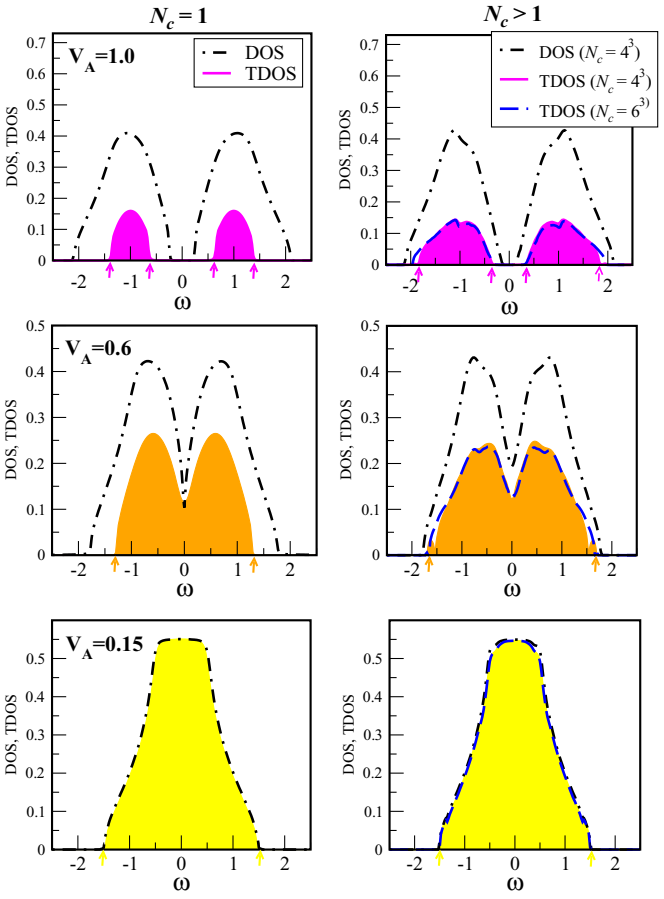

FIG. 4. (Color online) Diagonal-disorder case: The average density of states (dashed-dotted line) calculated within the DCA for $N_c = 1$ (left panel) and $N_c = 4^3$ (right panel) and the typical density of states shown as shaded regions for $N_c = 1$ (left panel) and $N_c = 4^3$ (right panel), and the dashed lines for $N_c = 6^3$ (right panel) are calculated within the TMDCA for diagonal disorder $t^{AA} = t^{BB} = t^{AB} = t^{BA} = 1$, $c_A = 0.5$, and various values of the local potential $V_A = -V_B$. The TDOS is presented for several cluster sizes $N_c = 1$, $N_c = 4^3$, and $N_c = 6^3$ in order to show its systematic convergence with N_c. The average DOS converges for cluster sizes beyond $N_c = 4^3$. The TDOS is finite for the extended states and zero when the states are localized. The mobility edges extracted from the vanishing of the TDOS are marked by the arrows (we show arrows for $N_c = 4^3$ only). The extended states region with a finite TDOS is always narrower for $N_c = 1$ as compared to the results of the $N_c > 1$ clusters, indicating that a single-site TMT tends to overemphasize the localized states.

our results for $N_c = 1$ (left panel) and $N_c > 1$ (right panel). To demonstrate a systematic convergence of the TDOS with increasing cluster size N_c, we present our data of the TDOS for $N_c = 1, 4^3, 6^3$. Notice that $N_c = 1$ results for the TDOS correspond to the single-site TMT of Dobrosavljević *et al.* [45], and for average DOS they correspond to the ordinary CPA. As expected [35,45], for small disorder ($V_A = 0.15$) there is not much difference between the DCA ($N_c = 4^3$) and the TMDCA ($N_c = 4^3$) or between the CPA and the TMT for the $N_c = 1$ results. However, there are subtle differences between the results for finite $N_c = 4^3$ and single site $N_c = 1$ clusters due to incorporation of spatial correlations. As the disorder strength V_A is increased ($V_A = 0.6$), the TDOS becomes smaller than the average DOS and is broader for the larger cluster. Moreover, the finite cluster introduces features in the DOS which are missing in the local $N_c = 1$ data. Regions where the TDOS is zero while the average DOS is finite indicate Anderson localized states, separated by the mobility edge (marked by arrows). For $N_c > 1$ these localized regions are wider, which indicates that the localization edge is driven to higher frequencies. This is a consequence of the tendency of nonlocal corrections to suppress localization. For even larger disorder $V_A = 1$, a gap opens in both the TDOS and the average DOS leading to the formation of four localization edges, but again the region of extended states is larger for the finite cluster, indicating that local TMT ($N_c = 1$) tends to underestimate the extended states region.

To further benchmark our results for the diagonal disorder, we show in Fig. 5 a comparison of the average and typical DOS calculated with the DCA and the TMDCA ($N_c = 4^3$) as compared with the KPM [47–50]. In the KPM analysis, instead of diagonalizing the Hamiltonian directly, the local DOS is expressed in terms of an infinite series of Chebyshev polynomials. In practice, the truncated series leads to Gibbs oscillations. The KPM damps these oscillations by a modification of the expansion coefficients. Following previous studies on the Anderson model, the Jackson kernel is used [48]. The details of the implementation are well discussed in Ref. [48]. The parameters used in the KPM calculations are listed in the caption of Fig. 5. As is evident from the plots, our TMDCA results reproduced those from the KPM nicely showing that our formalism offers a systematic way of studying the Anderson localization transition in binary-alloy systems. Such good agreement indicates a successful benchmarking of the TMDCA method [35].

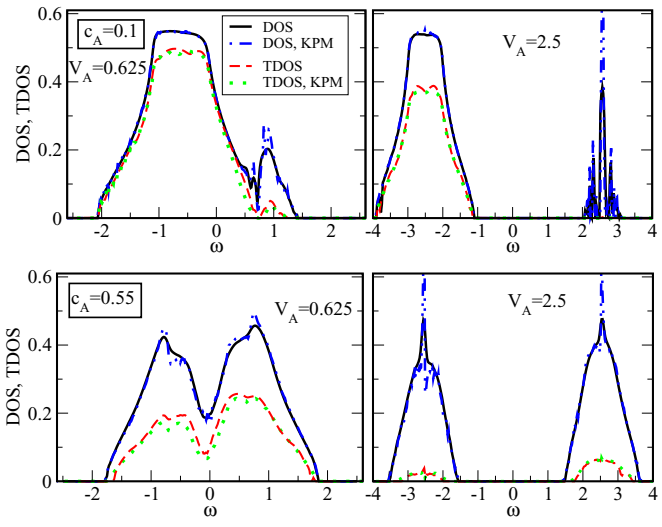

FIG. 5. (Color online) Diagonal-disorder case. Comparison of the average and typical DOS calculated with the DCA/TMDCA and kernel polynomial methods (KPMs) [47] for diagonal disorder with $t^{AA} = t^{BB} = t^{AB} = t^{BA} = 1$ at various values of local potential V_A and concentrations c_A for cluster size $N_c = 6^3$. The kernel polynomial method used 2048 moments on a 48^3 cubic lattice and 200 independent realizations generated with 32 sites randomly sampled from each realization.

Typical medium analysis of off-diagonal disorder

Next, we explore the effects of the off-diagonal disorder. In Fig. 6, we compare the typical TDOS from the TMDCA and average DOS from the DCA for several values of the diagonal-disorder strength V_A at fixed off-diagonal-disorder amplitudes $t^{AA} = 1.5$, $t^{BB} = 0.5$, and $t^{AB} = 1.0$. To show the effect of a finite cluster with respect to incorporation of nonlocal correlations, we present data for the single site $N_c = 1$ and finite clusters $N_c = 4^3$ and 5^3. The TMT ($N_c = 1$) again underestimates the extended states regime by having a narrower TDOS as compared to $N_c > 1$. We also see that the mobility edge defined by the vanishing of the TDOS (marked by arrows for $N_c = 4^3$) systematically converges with increasing cluster size N_c. For small disorder V_A, both the DOS and the TDOS are practically the same. However, as V_A increases, significant differences start to emerge. Increasing V_A leads to the gradual opening of the gap which is more pronounced in the $N_c = 1$ case and for smaller disorder $V_A = 0.6$ is partially filled for the $N_c > 1$ clusters. As compared to the diagonal-disorder case (cf. Fig. 4), the average DOS and TDOS become asymmetric with respect to zero frequency due to the off-diagonal randomness.

In Figs. 7 and 8 we present the disorder-energy phase diagram for both diagonal (Fig. 7) and off-diagonal (Fig. 8) disorders calculated using the single TMT ($N_c = 1$) and the nonlocal TMDCA ($N_c > 1$). To check the accuracy of the mobility edge trajectories extracted from our typical medium analysis, we compare our data with the results obtained with the TMM.

The TMM [13,51,52] is a well-established numerical method for calculating the correlation length and determining the mobility edge of the disorder Anderson model. Its main advantage is in its capability of capturing the effects from rather large system sizes. Thus, the TMM provides good data for a finite-size scaling analysis to capture the critical points and the corresponding exponents. In our calculations, the transmission of states down a three-dimensional bar of widths $M = [6,12]$ and length $L = 2 \times 10^4 M$ are studied by adding the products of the transfer matrices with random initial states. The multiplication of transfer matrices is numerically unstable. To avoid this instability, we orthogonalized the transfer-matrix product every five multiplications using a LAPACK QR decomposition [7]. The localization edge is obtained by calculating the Kramer-MacKinnon scaling parameter Λ_M [51]. This is a dimensionless quantity which should be invariant at the

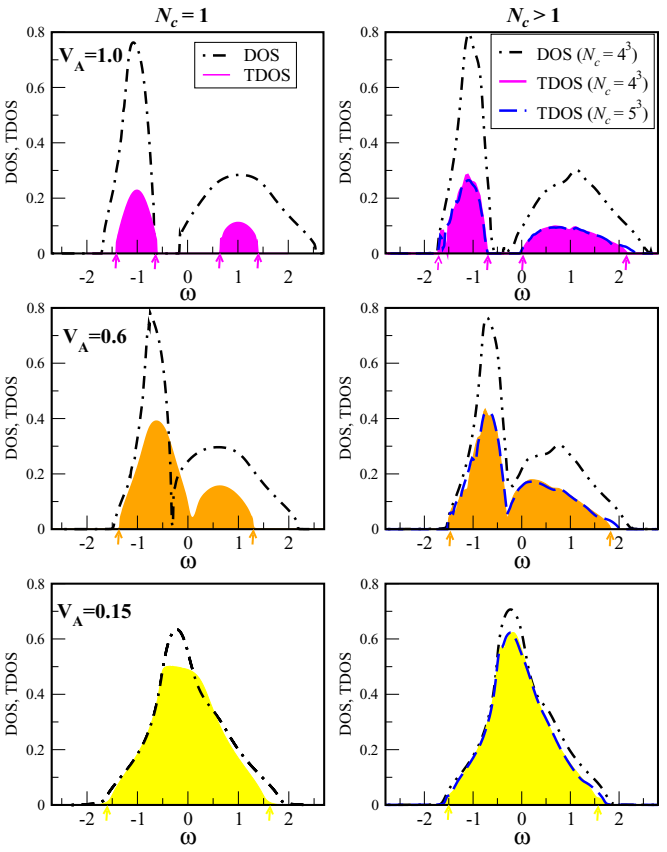

FIG. 6. (Color online) Off-diagonal-disorder case. The left panel displays results for $N_c = 1$, and the right panel displays results for $N_c > 1$. The average density of states (dashed-dotted line) and the typical density of states (shaded regions) for $N_c = 1$ (left panel), $N_c = 4^3$ (right panel), and blue dashed lines for $N_c = 5^3$ (left panel) for various values of the local potential V_A with off-diagonal-disorder parameters: $t^{AA} = 1.5$, $t^{BB} = 0.5$, $t^{AB} = 0.5(t^{AA} + t^{BB})$, and $c_A = 0.5$. As in Fig. 4, we show the TDOS for several cluster sizes $N_c = 1$, 4^3, and 6^3 in order to show its systematic convergence with increasing cluster size N_c. The average DOS converges for cluster sizes beyond $N_c = 4^3$. The TDOS is finite for the extended states and zero for the localized states. The mobility edges are extracted as described in Fig. 4.

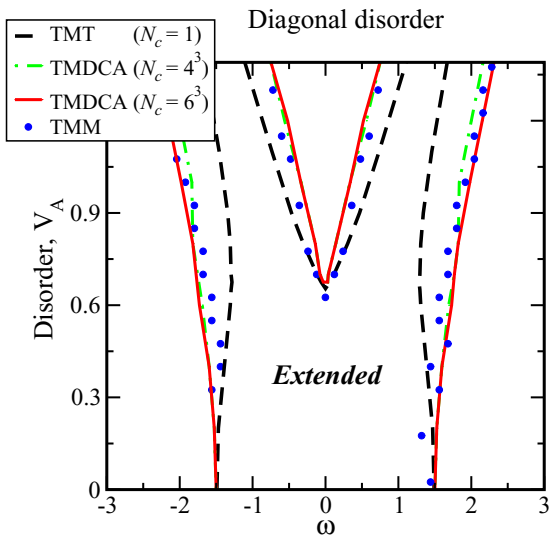

FIG. 7. (Color online) Disorder-energy phase diagram for the diagonal-disorder case. Parameters used are as follows: $t^{AA} = t^{BB} = t^{AB} = 1.0$, and $c_A = 0.5$. We compare the mobility edges obtained from the TMT $N_c = 1$ (black dashed line), TMDCA with $N_c = 4^3$ (green dot-dashed line) and $N_c = 6^3$ (red solid line), and the transfer-matrix method (TMM) (blue dotted line). The single site $N_c = 1$ results strongly underestimate the extended states region when compared with TMDCA results for $N_c > 1$. The mobility edges obtained from the finite cluster TMDCA ($N_c > 1$) show good agreement with those obtained from the TMM, in contrast to single-site TMT. See the text for parameters and details of the TMM implementation.

critical point, that is, Λ_M scales as a constant for $M \to \infty$ [52]. Thus, we determine the boundary of the localization transition vis-à-vis the critical disorder strength [53] by performing a linear fit to Λ_M vs M data: Localized states will have a negative slope and vise versa for extended states. The transfer-matrix method finite-size effects are larger for weak disorder where the states decay slowly with distance and so have large values of Λ_M that carry a large variance in the data. Notice that the CPA and the DCA do not suffer such finite-size effect limitations for small disorder and are in fact exact in this limit.

The mobility edges shown in Figs. 7 and 8 were extracted from the TDOS with boundaries being defined by zero TDOS. As can be seen in Figs. 7 and 8, although the single-site TMT does not change much under the effect of off-diagonal disorder, the TMDCA results are significantly modified. The bands for a larger cluster become highly asymmetric with significant widening of the A sub-band. The local $N_c = 1$ boundaries are narrower than those obtained for $N_c > 1$, indicating that the TMT strongly underestimates the extended states regime in both diagonal and off-diagonal disorders. On the other hand, comparing the mobility edge boundaries for $N_c > 1$ with those obtained using TMM, we find very good agreement. This again confirms the validity of our generalized TMDCA.

Next, we consider the effect of off-diagonal disorder for various concentrations c_A. In Fig. 9, we show the typical and average DOS for several values of c_A calculated with the TMDCA and the DCA, respectively. As expected, when $c_A \to 0$, we obtain a pure B sub-band contribution (the top panel). Upon gradual increase in the c_A concentration, the number of states in the A sub-band grows until the B sub-band becomes a minority for $c_A > 0.5$ and completely disappears at $c_A \to 1$ (the bottom panel). Again, we see that a finite cluster $N_c = 5^3$ provides a more accurate description (with finite details in DOS and broader regions of extended states in TDOS) in both average DOS and TDOS. The associated contour plots for the evolution of the TDOS in the concentration range of $0 \leqslant c_A \leqslant 1$ are shown in Fig. 10. The essence of these plots is to show the overall evolution of the typical DOS for a fixed local potential and off-diagonal-disorder parameters as a function of the concentration c_A. In the limit of $c_A \to 0$, only the B sub-band centered around $\omega = -V_A$ survives, and for $c_A \to 1$, only the A sub-band centered around $\omega = V_A$ is present. For intermediate concentrations, we clearly have contributions to the total typical density of states from both species as expected.

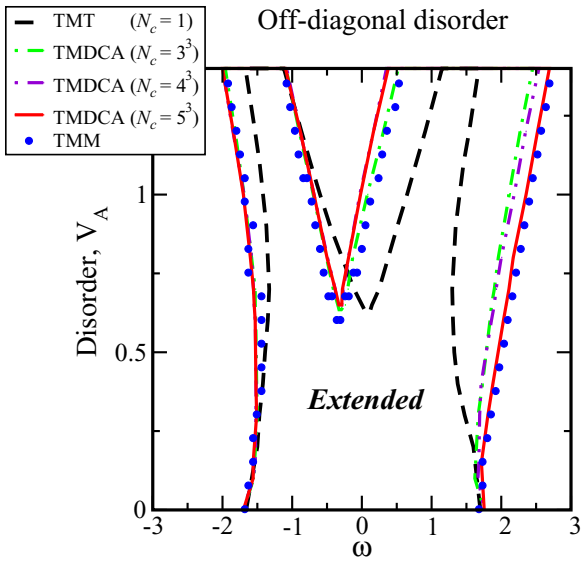

FIG. 8. (Color online) Disorder-energy phase diagram for the off-diagonal-disorder case. Parameters used are $t^{AA} = 1.5$, $t^{BB} = 0.5$, $t^{AB} = 1.0$, and $c_A = 0.5$. The mobility edges obtained from the TMT $N_c = 1$ (black dashed line), TMDCA $N_c = 3^3$ (green dot-dashed line), $N_c = 4^3$ (purple double-dot-dashed line) and $N_c = 5^3$ (red solid line), and the TMM (blue dotted line). The single site $N_c = 1$ strongly underestimates the extended states region especially for higher values of V_A. The mobility edges obtained from the finite cluster TMDCA ($N_c > 1$) converge gradually with increasing N_c and show good agreement with those obtained from the TMM, in contrast to single-site TMT. See the text for parameters and details of the TMM implementation.

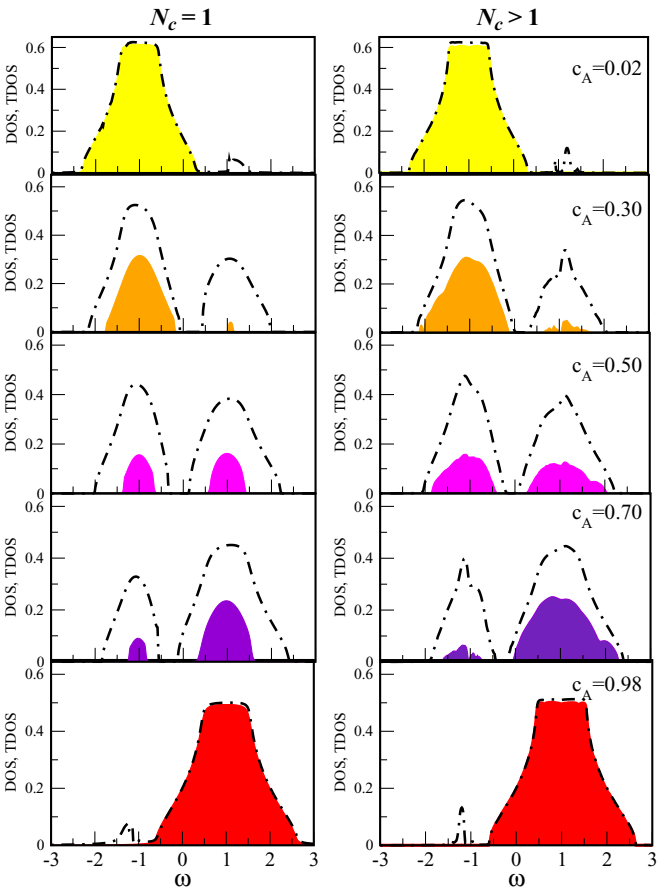

FIG. 9. (Color online) The average DOS (dot-dashed lines) and the typical DOS (shaded regions) for various values of the concentration c_A with off-diagonal-disorder parameters $t^{AA} = 1.1$, $t^{BB} = 0.9$, and $t^{AB} = 1.0$ at fixed local potential $V_A = 1.0$ for $N_c = 1$ (left panel) and $N_c = 5^3$ (right panel).

Finally, we would like to comment on the possible further development of the presented scheme. After certain generalizations our current implementation of the typical medium dynamical cluster approximation for off-diagonal disorder can serve as the natural formalism for multiband (multiorbital) systems [17]. Such an extension is crucial for studying disorder and localization effects in real materials. Further development towards this direction will be the subject of future papers.

IV. CONCLUSION

A proper theoretical description of disordered materials requires the inclusion of both diagonal and off-diagonal randomnesses. In this paper, we have extended the BEB single-site CPA scheme to a finite cluster DCA that incorporates the effect of nonlocal disorder. Applying the generalized DCA scheme to a single-band tight-binding Hamiltonian with configuration-dependent hopping amplitudes, we have considered the effects of nonlocal disorder and the interplay of diagonal and off-diagonal disorders on the average density of states. By comparing our results with those from exact numerical methods, we have established the accuracy of our method. We found that nonlocal multisite effects lead to the development of finite structures in the density of states and the partial filling of the gap at larger disorder. Utilizing the self-energy, we show as a function of increasing disorder strengths, the importance of a finite cluster in characterizing the Anderson localization transition. For small disorder the single-site and finite cluster results are essentially the same, indicating that the CPA is a good approximation in the small disorder regime. However, for a larger disorder we observe a significant momentum dependence in the self-energy resulting from the nonlocal correlations which are incorporated in the DCA.

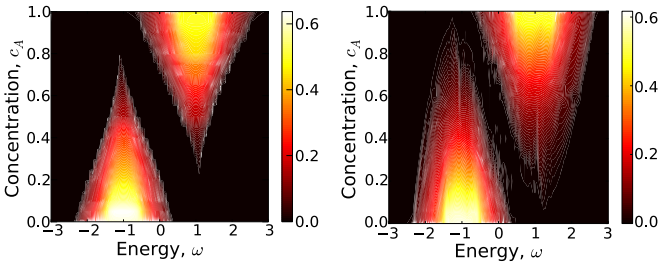

FIG. 10. (Color online) The evolution of the typical density of states for $N_c = 1$ (left panel) and $N_c = 5^3$ (right panel) with the change in the concentration $0 < c_A < 1$ at fixed diagonal- and off-diagonal-disorder parameters: $t^{AA} = 1.1$, $t^{BB} = 0.9$, $t^{AB} = 1.0$, and $V_A = 1.0$.

Electron localization for off-diagonal-disorder models from the typical medium perspective has been studied here. In this paper, we generalized the TMDCA to systems with both diagonal and off-diagonal disorders. Our developed method can quantitatively and qualitatively be used to study the effects of disorder on the electron localization, effectively for systems with both diagonal and off-diagonal randomnesses.

We demonstrate that within the TMDCA, the typical DOS vanishes for localized states and is finite for states which are extended. Employing the typical DOS as an order parameter for Anderson localization, we have constructed the disorder-energy phase diagram for systems with both diagonal and off-diagonal disorders. We have also demonstrated the inability of the single-site CPA and the TMT methods to accurately capture the localization and disorder effects in both the average and the typical DOS, respectively. We note that the single-site TMT, while being able to capture the behavior for the diagonal and off-diagonal disorders, strongly underestimates the extended regions. Also the TMT is less sensitive to the off-diagonal randomness with the mobility edges being only slightly modified as compared to the diagonal case. In contrast, the finite cluster TMDCA results are able to capture the considerable changes with a pronounced asymmetry of the extended state region in the disorder-energy phase diagram under the effect of the off-diagonal disorder as compared to the diagonal case. Most importantly, the TMDCA results are found to be in a quantitative agreement with the exact numerical results. Comparing our results with kernel polynomial, exact diagonalization, and transfer-matrix methods we find a remarkably good agreement with our extended DCA and TMDCA. We numerically accurately investigate the Anderson localization in systems with off-diagonal disorder within the framework of the typical medium analysis. We believe that the extended TMDCA scheme presents a powerful tool for treating both diagonal and off-diagonal disorders on equal footing and can be easily extended to study localization in multiband systems.

ACKNOWLEDGMENTS

We thank A. Gonis for useful discussions and directing us to the BEB formalism. We also thank S. Yang, W. Ku, and T. Berlijn for useful discussions. This work was supported by DOE SciDAC Grant No. DE-FC02-10ER25916 (M.J.) and BES CMCSN Grant No. DE-AC02-98CH10886 (H.T.). Additional support was provided by NSF EPSCoR Cooperative Agreement No. EPS-1003897 (H.T., C.E.E., C.M., and K.-M.T.) and NSF Grant No. OISE-0952300 (J.M.). This work used the Extreme Science and Engineering Discovery Environment (XSEDE), which is supported by National Science Foundation Grant No. ACI-1053575, the high performance computational resources provided by the Louisiana Optical Network Initiative (http://www.loni.org), and HPC@LSU computing.

[1] P. A. Lee and T. V. Ramakrishnan, Rev. Mod. Phys. **57**, 287 (1985).
[2] D. Belitz and T. R. Kirkpatrick, Rev. Mod. Phys. **66**, 261 (1994).
[3] P. W. Anderson, Phys. Rev. **109**, 1492 (1958).
[4] E. Abrahams, P. W. Anderson, D. C. Licciardello, and T. V. Ramakrishnan, Phys. Rev. Lett. **42**, 673 (1979).
[5] B. Bulka, B. Kramer, and A. MacKinnon, Z. Phys. B: Condens. Matter **60**, 13 (1985).
[6] B. Bulka, M. Schreibe, and B. Kramer, Z. Phys. B: Condens. Matter **66**, 21 (1987).
[7] K. Slevin and T. Ohtsuki, New J. Phys. **16**, 015012 (2014).
[8] K. Slevin and T. Ohtsuki, Phys. Rev. Lett. **78**, 4083 (1997).
[9] K. Slevin and T. Ohtsuki, Phys. Rev. Lett. **82**, 382 (1999).
[10] A. Rodriguez, L. J. Vasquez, K. Slevin, and R. A. Römer, Phys. Rev. Lett. **105**, 046403 (2010).
[11] A. Rodriguez, L. J. Vasquez, K. Slevin, and R. A. Römer, Phys. Rev. B **84**, 134209 (2011).
[12] T. Nakayama and K. Yakubo, *Fractal Concepts in Condensed Matter Physics* (Springer-Verlag, Berlin/Heidelberg, 2003).
[13] P. Markoš, Acta Phys. Slovaca **56**, 561 (2006).
[14] P. Markoš, J. Phys. A **33**, L393 (2000).
[15] A. Gonis, *Green Functions for Ordered and Disordered Systems* (North-Holland, Amsterdam, 1992).
[16] P. Soven, Phys. Rev. **156**, 809 (1967).
[17] K. Koepernik, B. Velický, R. Hayn, and H. Eschrig, Phys. Rev. B **58**, 6944 (1998).
[18] P. D. Antoniou and E. N. Economou, Phys. Rev. B **16**, 3768 (1977).
[19] K. Kumar, D. Kumar, and S. K. Josh, J. Phys.: Condens. Matter **10**, 1741 (1977).
[20] G. X. Tang and W. Nolting, Phys. Rev. B **73**, 024415 (2006).
[21] D. C. Licciardello and E. N. Economou, Phys. Rev. B **11**, 3697 (1975).
[22] G. Theodorou and M. H. Cohen, Phys. Rev. B **13**, 4597 (1976).
[23] E. R. Mucciolo and C. H. Lewenkopf, J. Phys.: Condens. Matter **22**, 273201 (2010).
[24] S.-J. Xiong and Y. Xiong, Phys. Rev. B **76**, 214204 (2007).
[25] A. Alam, B. Sanyal, and A. Mookerjee, Phys. Rev. B **86**, 085454 (2012).
[26] J. A. Blackman, D. M. Esterling, and N. F. Berk, Phys. Rev. B **4**, 2412 (1971).
[27] A. Gonis and J. W. Garland, Phys. Rev. B **18**, 3999 (1978).
[28] A. Gonis and J. W. Garland, Phys. Rev. B **16**, 1495 (1977).
[29] M. H. Hettler, A. N. Tahvildar-Zadeh, M. Jarrell, T. Pruschke, and H. R. Krishnamurthy, Phys. Rev. B **58**, R7475 (1998).
[30] M. H. Hettler, M. Mukherjee, M. Jarrell, and H. R. Krishnamurthy, Phys. Rev. B **61**, 12739 (2000).
[31] M. Jarrell and H. R. Krishnamurthy, Phys. Rev. B **63**, 125102 (2001).
[32] H. Shiba, Prog. Theor. Phys. **46**, 77 (1971).
[33] A. Brezini, M. Sebbani, and L. Dahmani, Phys. Status Solidi B **137**, 667 (1986).
[34] F. Hamdache and A. Brezini, Phys. Status Solidi B **172**, 635 (1992).
[35] C. E. Ekuma, H. Terletska, K.-M. Tam, Z.-Y. Meng, J. Moreno, and M. Jarrell, Phys. Rev. B **89**, 081107 (2014).
[36] D. J. Thouless, Phys. Rep. **13**, 93 (1974).

[37] A. Abou-Chacra, D. J. Thouless, and P. W. Anderson, J. Phys. C **6**, 1734 (1973).
[38] P. W. Anderson, Rev. Mod. Phys. **50**, 191 (1978).
[39] A. D. Mirlin and Y. V. Fyodorov, Phys. Rev. Lett. **72**, 526 (1994).
[40] K. Byczuk, W. Hofstetter, and D. Vollhardt, Int. J. Mod. Phys. B **24**, 1727 (2010).
[41] G. Schubert, J. Schleede, K. Byczuk, H. Fehske, and D. Vollhardt, Phys. Rev. B **81**, 155106 (2010).
[42] M. Janssen, Phys. Rep. **295**, 1 (1998).
[43] *Log-Normal Distribution—Theory and Applications*, edited by E. Crow and K. Shimizu (Dekker, New York, 1988).
[44] B. Derrida, Phys. Rep. **103**, 29 (1984).
[45] V. Dobrosavljević, A. A. Pastor, and B. K. Nikolić, Europhys. Lett. **62**, 76 (2003).
[46] A. Alvermann, G. Schubert, A. Weiße, F. X. Bronold, and H. Fehske, Physica B **359**, 789 (2005).
[47] G. Schubert and H. Fehske, in *Quantum and Semi-Classical Percolation and Breakdown in Disordered Solids*, edited by B. K. Chakrabarti, K. K. Bardhan, and A. K. Sen, Lecture Notes in Physics Vol. 762 (Springer, Berlin/Heidelberg, 2009), pp. 1–28.
[48] A. Weiße, G. Wellein, A. Alvermann, and H. Fehske, Rev. Mod. Phys. **78**, 275 (2006).
[49] G. Schubert, A. Weiße, and H. Fehske, Phys. Rev. B **71**, 045126 (2005).
[50] G. Schubert and H. Fehske, Phys. Rev. B **77**, 245130 (2008).
[51] A. MacKinnon and B. Kramer, Z. Phys. B: Condens. Matter **53**, 1 (1983).
[52] B. Kramer, A. MacKinnon, T. Ohtsuki, and K. Slevin, Int. J. Mod. Phys. B **24**, 1841 (2010).
[53] I. V. Plyushchay, R. A. Römer, and M. Schreiber, Phys. Rev. B **68**, 064201 (2003).